Applied Physics B manuscript No.
(will be inserted by the editor)

Birefringence of interferential mirrors at normal incidence

Experimental and computational study

F. Bielsa[1], A. Dupays[2,3], M. Fouché[2,3], R. Battesti[1], C. Robilliard[2,3], C. Rizzo[2,3]

[1] Laboratoire National des Champs Magnétiques Intenses (UPR 3228, CNRS-INSA-UJF-UPS), F-31400 Toulouse Cedex, France
[2] Université de Toulouse, UPS, Laboratoire Collisions Agrégats Réactivité, IRSAMC, F-31062 Toulouse, France
[3] CNRS, UMR 5589, F-31062 Toulouse, France

Received: date / Revised version: date

arXiv:0907.4007v1 [physics.optics] 23 Jul 2009

Abstract In this paper we present a review of the existing data on interferential mirror birefringence. We also report new measurements of two sets of mirrors that confirm that mirror phase retardation per reflection decreases when mirror reflectivity increases. We finally developed a computational code to calculate the expected phase retardation per reflection as a function of the total number of layers constituting the mirror. Different cases have been studied and we have compared computational results with the trend of the experimental data. Our study indicates that the origin of the mirror intrinsic birefringence can be ascribed to the reflecting layers close to the substrate.

1 Introduction

In the last decades, high reflectivity interferential mirrors have been widely used in optical cavities to measure small light polarization variations induced by the propagation in a weakly anisotropic medium such as in parity violation experiments [1,2] or in vacuum magnetic birefringence experiments [3,4,5]. Mirrors themselves are birefringent and this is manifestly a problem for such a kind of applications because they induce a phase retardation [6] which superimposes to the signal to be measured. This birefringence is due to off-normal incidence and/or to intrinsic birefringence of the mirror coatings. In the case of Fabry-Perot cavities the incidence on the mirrors is normal. In this paper we focus on this type of device, thus on birefringence due to the mirror coatings.

Interferential mirrors are composed of a stack of slabs deposited on a substrate. One slab corresponds to a low-index layer and a high-index layer with an optical thickness $\lambda/4$ for each layer, where λ is the light wavelength for which the mirror reflectivity is optimized. While non birefringent stratified media are discussed in textbooks [17], and films with a non trivial dielectric tensor have been treated in literature (see e.g. [18]), as far as we know, the origin of the mirror birefringence is unknown, and a detailed study of the problem does not exist. In ref. [19] computational results are given in the hypothesis that the birefringence is due to only one layer, in particular the uppermost. The author notices that the phase retardation effect diminishes as he moves the only phase retardation layer down the stack. In ref. [15] measurements of the mirror phase retardation as a function of time and of laser power in the Fabry-Perot cavity have been performed. The authors suggest that mirror birefringence may be photoinduced, at least partly.

In this paper we present a review of the existing data on interferential mirror phase retardation. We show that the data indicate that the phase retardation per reflection decreases when the mirror reflectivity becomes better and better i.e. when the total number of layers increases. We also report new measurements of two sets of mirrors that confirm this trend. We finally developed a computational code to calculate the expected phase retardation per reflection as a function of the total number of layers. Different cases have been studied going from a fixed birefringence for each layer to a random birefringence for each layer. We finally compare computational results with the trend of the experimental data. Our study indicates that the origin of the mirror intrinsic birefringence can be ascribed to the reflecting layers close to the substrate.

2 Experimental study

Birefringence of interferential mirrors have been measured and reported by several authors [7,8,9,10,11,12, 13,14,15]. The phase retardation per reflection ranges between a few 10^{-7} rad to 10^{-3} for values of $(1-R)$ going from a few 10^{-5} to 10^{-2}, where R is the mirror

Send offprint requests to: carlo.rizzo@irsamc.ups-tlse.fr

reflectivity. All the measurements have been conducted using an optical cavity except one [9], where the ellipticity acquired after a single reflection was directly measured. Optical cavities are usually absolutely necessary to accumulate the effect and thus to allow to measure very small phase retardations. Whereas a multipass cavity has been used in refs. [7,8], a Fabry-Perot cavity is used in refs. [10,11,12,13,14]. In the following section, the published data are presented in details, in chronological order. These studies were always motivated by measurements of small phase retardation such as parity violation experiments [1,2] or vacuum magnetic birefringence experiment [3].

2.1 Review of published data

The first study of intrinsic phase retardation of interferential mirrors dates from 1982 [7]. Measurements have been conducted using a multipass cavity made of two spherical mirrors between which the light beam bounces many times forwards and backwards under quasinormal incidence. Intrinsic phase retardation is therefore superimposed to the off-normal incidence phase retardation but this has also been evaluated by the authors. The light beam does not hit the same point of the mirror after a round trip. Thus the measurement of phase retardation per reflection gives a value averaged on the mirror surface. The mirrors have been manufactured by Spectra-Physics, Inc. (Mountain View, CA, USA), and their reflectivity R is 0.998 at λ =540 nm. Intrinsic phase retardation typically varies between 2 and 4×10^{-4} rad per reflection. Among the 19 mirrors analyzed, two exceptions with phase retardation less than 10^{-6} rad per reflection have been found. The authors called this a "happy accident".

A few years later a new study was again performed using a multipass cavity [8]. A set of 5 mirrors manufactured by MTO, Palaiseau, France, has been analyzed. The authors did not give explicitly the reflectivity of the mirrors, but they have reported that at $\lambda = 514.5$ nm and after about 250 reflections the light intensity is reduced to $1/e$. We can deduce that $(1-R) = 0.004$. From their measurements, intrinsic phase retardation varies between 3.0×10^{-5} and 2.2×10^{-4} rad per reflection.

The next study was performed in 1993 [9] using multipass cavities. Only one mirror has been analyzed but this time the phase retardation has been measured directly after only one reflection. The mirror had a reflectivity of 0.9983 at 633 nm. It was coated by the Laboratory of Laser Energetics of the University of Rochester. The authors were able to measure the intrinsic phase retardation and the phase retardation axis direction of the mirror in different points of the surface. They could therefore draw a map of the intrinsic phase retardation showing a clear rotational pattern. The intrinsic phase retardation per reflection ranged between 3 to 6.2×10^{-4} rad, while the axis direction ranged between 9 and -13 degrees. To test that the origin of such an anisotropy was not due to the substrate, the authors have measured the phase retardation when the light was reflected on the backsurface of the mirror. They obtained a result compatible with zero within the experimental error.

In 1995 the first measurement using a Fabry-Perot cavity was reported [10]. In this type of interferometer the incidence on the mirrors is strictly normal, and off-normal phase retardation vanishes. The mirror reflectivity can be inferred by the cavity finesse $F = 6600$ given by the authors at $\lambda = 633$ nm: $R = 1-\pi/F = 0.999524$. The reported values of phase retardation per reflection are 1.0×10^{-6} and 4.4×10^{-6} rad. Besides, their study allows to conclude that the birefringence is not due to the mirror mounts.

In 1996, a new intrinsic phase retardation of a mirror is reported [11]. The Fabry-Perot cavity finesse was 300 at $\lambda = 633$ nm, and we can therefore infer that $R = 0.9895$. The measured phase retardation per reflection is 1.2×10^{-3} rad.

For the next value reported in ref. [12], a Fabry-Perot was again used. The mirrors have been manufactured by Research Electro-Optics Inc., Boulder, Colorado, USA. The Fabry-Perot cavity finesse was 125600 at $\lambda = 540$ nm, and the inferred reflectivity is $R = 0.999975$. The value of the phase retardation per reflection is given for only one mirror and corresponds to 3×10^{-6} rad.

In 1997 two works have been published in the same journal issue [13,14] concerning mirror intrinsic phase retardation. In ref. [13] two mirrors constituting a Fabry-Perot cavity have been characterized. The average value of the reported reflectivity was $R = 0.9988$ at $\lambda = 633$ nm. The measured phase retardation per reflection was 4.2×10^{-4} rad and 1.04×10^{-3} rad. In ref. [14], the reflectivity was $R = 0.999969$ at $\lambda = 1064$ nm and they have been manufactured by Research Electro-Optics Inc., Boulder, Colorado, USA. The measured value for three mirrors over four was between 3.7 and 12×10^{-7} rad, while the last mirror was a "happy accident" with a phase retardation per reflection smaller than 10^{-7} rad.

Finally in 2000, a new measurement is reported [15]. Measurements have been done on a Fabry-Perot cavity, looking at frequency shift of the resonance line of the cavity due to mirror phase retardation. The Fabry-Perot cavity finesse was about 40 000 at $\lambda = 633$ nm, corresponding to $R = 0.999923$, and the phase retardation per reflection 1.8×10^{-6} rad. The authors have also showed that the measured phase retardation could be changed by several percents by appropriately injecting more power in the cavity. Phase retardation relaxed down to the average value several seconds after the perturbation.

In table 1 we summarize the existing data on mirror intrinsic phase retardation per reflection. We give the reference number, the value of the reflectivity R, the measured value of the phase retardation per reflection

$\delta_{\rm M}$, the number of characterized mirrors $N_{\rm mirrors}$, and finally the light wavelength λ for which the mirror reflectivity was optimized. We give the minimum and the maximum value for $\delta_{\rm M}$ when several mirrors have been analyzed in the same reference. In the case of ref. [9], where a single mirror has been studied but in several points of its surface, we give the dispersion of the reported values.

Table 1 Review of published data.

ref.	R	$\delta_{\rm M}$ (rad)	$N_{\rm mirrors}$	λ (nm)
[7]	0.998	$(2-4)\times10^{-4}$	17	540
		$<10^{-6}$	2	540
[8]	0.996	$(3-22)\times10^{-5}$	5	514
[9]	0.9983	$(3-6.2)\times10^{-4}$	1	633
[10]	0.999524	$(1-4.4)\times10^{-6}$	2	633
[11]	0.9895	1.2×10^{-3}	1	633
[12]	0.999975	3×10^{-6}	1	540
[13]	0.9988	$(4.2-10.4)\times10^{-4}$	2	633
[14]	0.999969	$(7.4-24)\times10^{-7}$	3	1064
		$<10^{-7}$	1	1064
[15]	0.999923	1.8×10^{-6}	1	633

2.2 Our new measurements

In this paragraph we report new measurements of two different sets of mirror performed in the framework of the BMV experiment [22] which goal is to measure vacuum magnetic birefringence. As in the previous attempts to measure such a weak quantity [3,4,5], mirror intrinsic phase retardation is a source of noise limiting the sensitivity of the apparatus. Moreover, since signal detection in the BMV experiment corresponds to a homodyne technique, the ellipticity Γ induced on the linearly polarized laser beam by the Fabry-Perot cavity overall phase retardation is used as a D.C. carrier. To reach a shot noise limited sensitivity, one needs Γ to be as small as possible [22], implying that the phase retardation axis of the two mirrors constituting the cavity have to be aligned.

To measure the mirror intrinsic phase retardation, our experimental method is based on the ones described in details in ref. [10,14]. More details on our experimental setup can be found in ref. [22]. Briefly, 30 mW of a linearly polarized Nd:YAG ($\lambda = 1064$ nm) laser beam is injected into a Fabry-Perot cavity. This laser is locked to the cavity resonance frequency using the Pound-Drever-Hall method [23]. The beam transmitted by the cavity is then analyzed by a polarizer crossed at maximum extinction and collected by a low noise photodiode with a noise equivalent power of $0.25\,{\rm pW}/\sqrt{\rm Hz}$. Polarizer extinction is $(4\pm2)\times10^{-7}$ which is always much lower than the ellipticity we measure.

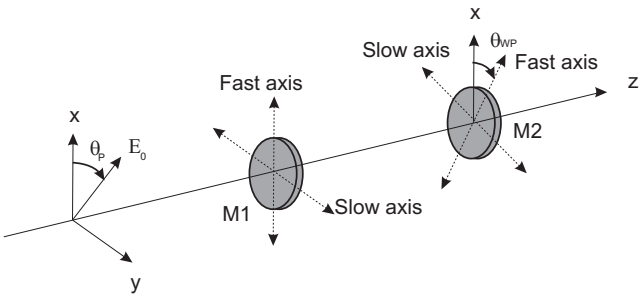


Fig. 1 Principle of the experiment: a linearly polarized laser beam is injected into a Fabry-Perot cavity (mirrors M1 and M2). The polarization is then analyzed outside of the cavity.

As shown on Fig. 1, both mirrors are schematized as two ideal waveplates with phase retardation δ_1 and δ_2. Thus the phase retardation per reflection of each mirror we want to measure corresponds to $2\delta_1$ and $2\delta_2$. For the sake of simplicity the angle indicating the direction of the phase retardation axis of the first mirror is taken as zero. The angle between the phase retardation axis of the two mirrors is $\theta_{\rm WP}$. For $\delta_1, \delta_2 \ll 1$, combination of both waveplates gives a single waveplate of phase retardation [14]:

$$\delta_{\rm EQ} = \sqrt{\left((\delta_1-\delta_2\right)^2 + 4\delta_1\delta_2\cos^2\theta_{\rm WP}}, \qquad (1)$$

and with a fast axis at an angle with respect to the x axis given by:

$$\cos 2\theta_{\rm EQ} = \frac{\frac{\delta_1}{\delta_2} + \cos 2\theta_{\rm WP}}{\sqrt{\left(\frac{\delta_1}{\delta_2}-1\right)^2 + 4\frac{\delta_1}{\delta_2}cos^2\theta_{\rm WP}}}. \qquad (2)$$

The Fabry-Perot cavity corresponds to a waveplate with a phase retardation δ related to $\delta_{\rm EQ}$ as follows :

$$\delta = \frac{2F}{\pi}\delta_{\rm EQ}, \qquad (3)$$

where F is the cavity finesse. Finally, the intensity transmitted by the analyzer over the incident intensity is equal to the square of the ellipticity ψ induced by the cavity mirrors. This ellipticity is given by [14]:

$$\psi^2 = \frac{\delta^2}{4}\sin^2(2(\theta_{\rm P}-\theta_{\rm EQ})), \qquad (4)$$

with $\theta_{\rm P}$ the angle indicating the direction of the light polarization with respect to the x axis. Thus, by measuring the intensity transmitted by the analyzer as a function of $\theta_{\rm WP}$ and for different value of $\theta_{\rm P}$, we are able to calculate the phase retardation of both mirrors.

Two different sets of mirrors have been tested. The first one is constituted by two one inch diameter spherical mirrors, 6 m radius of curvature, BK7 substrate, manufactured by Laseroptik GmbH, Garbsen (Germany). The reflectivity at $\lambda = 1064$ nm is 0.999396 corresponding to a cavity finesse of 5200 and the transmission of the

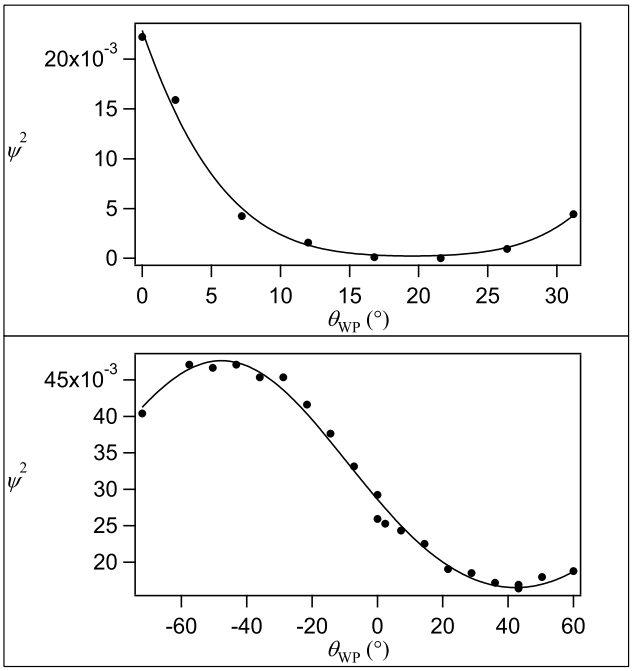


Fig. 2 Experimental values of the square of the ellipticity ψ as a function of the angle between the phase retardation axis of the cavity mirrors (see table 2). Data are fitted using Eq. (4). Upper curve: the mirrors reflectivity is 0.999396. Lower curve: the mirrors reflectivity is 0.999972.

cavity is about 20 %. The second set of mirrors is constituted by three one inch diameter spherical mirrors, 8 m radius of curvature, BK7 substrate, manufactured by Layertec GmbH, Mellingen (Germany). The reflectivity at $\lambda = 1064$ nm is 0.999972 corresponding to a cavity finesse of about 110000. According to the manufacturer, mirror losses are lower than 100 ppm and the overall measured transmission of the cavity is about 3 %.

The square of the ellipticity ψ induced by the cavity as a function of the angle between the phase retardation axis of the two mirrors is plotted in Fig. 2. Experimental values are fitted using Eq. (4). The deduced mirror intrinsic phase retardation per reflection is presented in Table 2 for each mirror.

Table 2 Mirror intrinsic phase retardation.

R	δ_M (rad)	No.	λ (nm)
0.999396	$(5.8 \pm 0.4) \times 10^{-4}$	1	1064
	$(3.4 \pm 0.4) \times 10^{-4}$	2	
0.999972	$(9.8 \pm 0.4) \times 10^{-6}$	1	1064
	$(2.6 \pm 0.4) \times 10^{-6}$	2	
	$(1 \pm 0.4) \times 10^{-6}$	3	

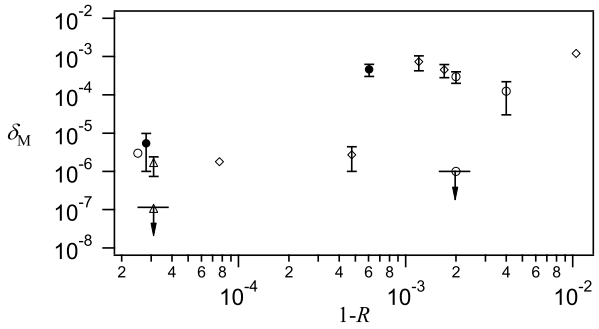


Fig. 3 Summary of all the published data and the data obtained in this work with mirror intrinsic phase retardation δ_M versus $(1 - R)$. The symbols represent the wavelength for which the mirror reflectivity was optimized ($\circ$: 540 nm, $\diamond$: 633 nm, $\triangle$: 1064 nm, $\bullet$: our work). Errors bars correspond to the minimum and the maximum value when several mirrors have been analyzed. Arrows represent mirrors for which the phase retardation was smaller than the apparatus sensitivity. The trend of the whole points shows that the intrinsic phase retardation decreases by 3 orders of magnitude as $(1 - R)$ decreases by almost 3 orders of magnitude.

2.3 Summary

All the published data together with the data obtained in this work are plotted as a function of $(1-R)$ on Fig. 3. When only one mirror has been tested, the corresponding point has no error bars. When different mirrors have been measured the data point have error bars. These error bars do not represent the measurement error for one mirror (typically 10%) but the dispersion of the measured value for the whole set of mirrors. Arrows represent mirrors for which the phase retardation was smaller than the apparatus sensitivity (see table 1 and 2). Dots represent the new measurements reported in this work at $\lambda = 1064$ nm.

Published data plotted on Fig. 3 clearly show that the higher the reflectivity i.e. the lower the value of $(1 - R)$, the lower the phase retardation per reflection. More precisely, the intrinsic phase retardation decreases by 3 orders of magnitude as $(1 - R)$ decreases by almost 3 orders of magnitude. Our new measurements perfectly confirm this trend.

3 Computational study

The understanding of the origin of the experimental data trend is crucial if one wants to control the manufacture to obtain birefringence free interferential mirrors. We have therefore developed a computer code that can simulate the behavior of an interferential mirror made by an arbitrary number of layers each one with its own arbitrary phase retardation and arbitrary retardation axis. Our goal was to find a configuration of layers, as simple as possible, that could reproduce the experimental trend

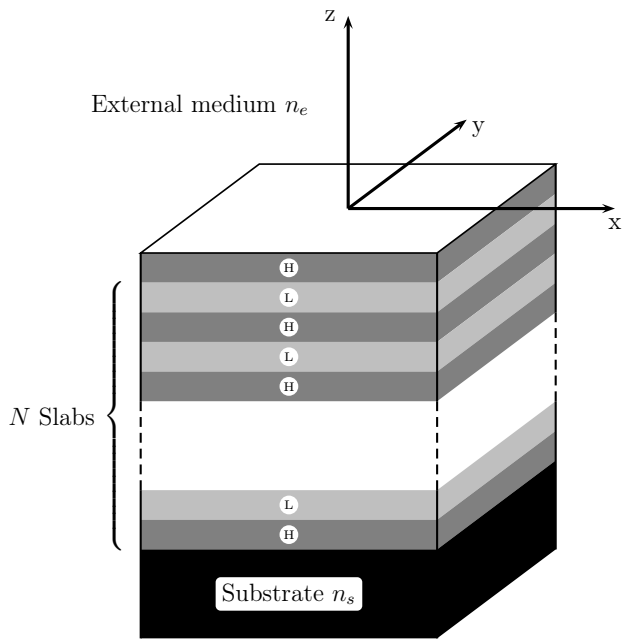


Fig. 4 Interferential mirror. It consists of an "odd stack" of slabs deposited on a substrate.

and give a first indication to experimentalists to test in further studies.

3.1 Interferential mirrors

Interferential mirrors are made by a stack of slabs of an optical thickness of $\lambda/2$ as shown on Fig. 4, where λ is the light wavelength for which the mirror reflectivity is optimized. Each slab is composed by a low-index layer $n_{\rm L}$ and a high-index layer $n_{\rm H}$. Each layer has an optical thickness of $\lambda/4$. Typically, $n_{\rm L}$ is around 1.5 and $n_{\rm H}$ is higher than 2.0. The substrate is usually fused silica or Zerodur, and a $\lambda/2$ coating of $Si0_2$ protects the reflecting surface of the mirror. Obviously, construction details are not shared publicly by manufacturers (see e.g. the paragraph on mirror manufacture in ref. [16]).

In the case of what is called an "odd stack" i.e. N slabs of a high-index layer and a low-index layer plus one high-index layer ($2N+1$ layers), the mirror reflectivity R can be written as [17]:

$$R = \left[\frac{1 - \left(\frac{n_{\rm H}}{n_{\rm s}}\right)^2 \left(\frac{n_{\rm H}}{n_{\rm L}}\right)^{2N}}{1 + \left(\frac{n_{\rm H}}{n_{\rm s}}\right)^2 \left(\frac{n_{\rm H}}{n_{\rm L}}\right)^{2N}} \right]^2 \tag{5}$$

where $n_{\rm s}$ is the index of refraction of the substrate. Typically to obtain a reflectivity $R \simeq 0.999999$ one needs about 20 pairs of quarter-wavelength layers of materials such as SiO2 and either TiO_2 or TaO_5, while 10 pairs are sufficient to obtain $R \simeq 0.999$.

3.2 Methods

The model multilayer we used for our calculations consists of a stack of slabs placed between two semi-infinite media of refractive indices $n_{\rm e}$ (the external medium) and $n_{\rm s}$ (the substrate). The coordinate system used to reference the multilayer axes is shown in Fig. 4.

Each birefringent layer is uniaxial. For the jth layer extending from $z = z_j$ to $z = z_{j+1}$ we denote by θ_{j+1} the angle between the principal axis of the birefringent medium and the reference frame and by $d_j = z_{j+1} - z_j$ its thickness (see Fig. 5).

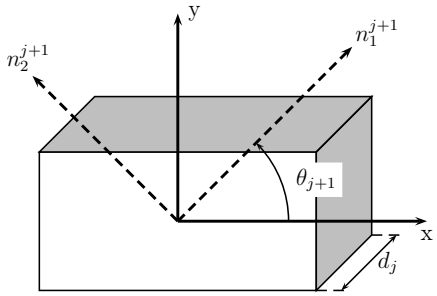


Fig. 5 Angle between the principal axis of the birefringent medium and the reference frame.

In the reference frame, the dielectric tensor of this layer is then given by

$$\epsilon^{j+1} = R^{-1}(\theta_{j+1}) \begin{pmatrix} \epsilon_1^{j+1} & 0 \\ 0 & \epsilon_2^{j+1} \end{pmatrix} R(\theta_{j+1}) \tag{6}$$

where $R(\theta)$ is the standard rotation matrix :

$$R(\theta) = \begin{pmatrix} \cos\theta & \sin\theta \\ -\sin\theta & \cos\theta \end{pmatrix}. \tag{7}$$

For a low-index layer, we have

$$\begin{cases} n_1^{j+1} = \sqrt{\epsilon_1^{j+1}/\epsilon_0} = n_{\rm L} + \delta n_{\rm L} \\ n_2^{j+1} = \sqrt{\epsilon_2^{j+1}/\epsilon_0} = n_{\rm L} \end{cases} \tag{8}$$

and for a high-index layer

$$\begin{cases} n_1^{j+1} = \sqrt{\epsilon_1^{j+1}/\epsilon_0} = n_{\rm H} + \delta n_{\rm H} \\ n_2^{j+1} = \sqrt{\epsilon_2^{j+1}/\epsilon_0} = n_{\rm H} \end{cases} \tag{9}$$

where ϵ_0 is the vacuum permeability and $n_{\rm L}, n_{\rm H}$ stand for refractive indices of similar but no-birefringent layers with an optical thickness of $\lambda/4$, so that $n_{1,2}^{j+1} d_j = \lambda/4$.

Let us now consider a transverse electric polarized plane monochromatic wave normally incident upon this model mirror. The solution of the Maxwell's equations for the electric field can be expressed as a superposition of the forward and backward propagating waves along

each reference direction x and y. In the external medium, we have

$$E_x = A^{+}_{\mathrm{e},x} \exp\{i(k_{\mathrm{e},x} z - \omega t)\} + A^{-}_{\mathrm{e},x} \exp\{i(-k_{\mathrm{e},x} z - \omega t)\} \quad (10)$$

for the x component and

$$E_y = A^{+}_{e,y} \exp\{i(k_{\mathrm{e},y} z - \omega t)\} + A^{-}_{\mathrm{e},y} \exp\{i(-k_{\mathrm{e},y} z - \omega t)\} \quad (11)$$

for the y component, where $\omega = 2\pi/\lambda$ and

$$k_{\mathrm{e},x} = k_{\mathrm{e},y} = \frac{\omega}{c} n_{\mathrm{e}} \quad (12)$$

with c the light velocity in vacuum. In the same way, the electric field in the substrate is written as

$$E_x = A^{+}_{\mathrm{s},x} \exp\{i(k_{\mathrm{s},x}(z - z_{2N+1}) - \omega t)\} + A^{-}_{\mathrm{s},x} \exp\{i(-k_{\mathrm{s},x}(z - z_{2N+1}) - \omega t)\} \quad (13)$$

for the x component and

$$E_y = A^{+}_{\mathrm{s},y} \exp\{i(k_{\mathrm{s},y}(z - z_{2N+1}) - \omega t)\} + A^{-}_{\mathrm{s},y} \exp\{i(-k_{\mathrm{s},y}(z - z_{2N+1}) - \omega t)\} \quad (14)$$

for the y component, where

$$k_{\mathrm{s},x} = k_{\mathrm{s},y} = \frac{\omega}{c} n_{\mathrm{s}}. \quad (15)$$

Using the characteristic matrix method [17], we have

$$\begin{pmatrix} A^{+}_{\mathrm{e},x} \\ A^{-}_{\mathrm{e},x} \\ A^{+}_{\mathrm{e},y} \\ A^{-}_{\mathrm{e},y} \end{pmatrix} = M \begin{pmatrix} A^{+}_{\mathrm{s},x} \\ A^{-}_{\mathrm{s},x} \\ A^{+}_{\mathrm{s},y} \\ A^{-}_{\mathrm{s},y} \end{pmatrix} \quad (16)$$

where M is a 4×4 matrix called the characteristic matrix of the multilayer. This matrix can be calculated step by step by solving numerically a 4×4 linear system of equations corresponding to the appropriate boundary conditions that must be fulfilled by the electric field at the interface between two adjacent layers. Noting that $A^{-}_{\mathrm{s},x} = A^{-}_{\mathrm{s},y} = 0$ and taking $A^{+}_{\mathrm{e},x} = 1$ and $A^{+}_{\mathrm{e},y} = 0$, we get

$$A^{-}_{\mathrm{e},x} = \frac{M_{21}}{\left(M_{11} - \frac{M_{13}M_{31}}{M_{33}}\right)} - \frac{M_{23}M_{31}}{M_{33}\left(M_{11} - \frac{M_{13}M_{31}}{M_{33}}\right)} \quad (17)$$

$$A^{-}_{\mathrm{e},y} = \frac{M_{41}}{\left(M_{11} - \frac{M_{13}M_{31}}{M_{33}}\right)} - \frac{M_{43}M_{31}}{M_{33}\left(M_{11} - \frac{M_{13}M_{31}}{M_{33}}\right)} \quad (18)$$

The induced ellipticity per reflection ψ_{M} is then given by

$$\tan\psi_{\mathrm{M}} = \frac{|A^{-}_{\mathrm{e},y}|}{|A^{-}_{\mathrm{e},x}|}. \quad (19)$$

Since measured phase retardations presented in the previous section are small, we only consider small birefringence. To fully reproduce the experimental technique we calculate ψ_{M} as a function of the angle between the polarization and the birefringent axis of the simulated mirror. We checked that it behaves as a standard wave plate from which we can extract the intrinsic phase retardation δ_{M}.

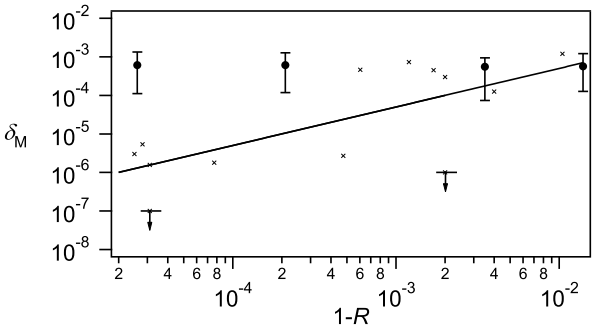


Fig. 6 Two different numerical calculations for the induced phase retardation per reflection as a function of $(1 - R)$. Solid curve : birefringence only for the first layer just after the substrate. Dots with error bars : calculation with random birefringence per each layer. Crosses : measurements plotted in Fig. 3.

3.3 Results

Using the code based on the methods detailed in the previous section, we have simulated several simple configurations. In the trivial case in which every layer gives the same contribution to the total effect, the straightforward result was that phase retardation per reflection increases with the number of layers i.e. with the mirror reflectivity. Random phase retardation and axis orientation per layer has also been tested varying the range of variation of these two parameters. No result similar to the experimental trend has been obtained. The configurations which can reproduce this trend are the ones in which the birefringent layers are only the ones close to the substrate.

Figure 6 presents two different numerical calculations for the induced phase retardation per reflection as a function of $(1 - R)$ where R is the multilayer reflectivity we got from our simulations. Crosses represent the measurements plotted in Fig. 3. To match these experimental data, we have chosen the parameters of our simulations such that numerical results reproduce the experimental data for the highest $(1 - R)$ available value. Dots with error bars correspond to the result of random calculations with $\delta n_{\mathrm{L(H)}}$ (resp. θ_j) randomly distributed inside the interval $[0, 0.001]$ (resp. $[-\pi, \pi]$) for each layer. The error bar for each point corresponds to the dispersion obtained with 10 tries. This result does not reproduce the experimental data. On the other hand, the solid curve has been obtained by including birefringence only for the layer lying directly on the substrate. The parameters we used are: $\delta n_{\mathrm{H}} = 0.13$ for the $(2N + 1)$th layer (zero for the others). This result reproduces quite well the trend of the experimental data i.e. the intrinsic phase retardation decreases by 3 orders of magnitude as $(1 - R)$ decreases by 3 orders of magnitude.

4 Conclusion

Existing experimental data on interferential mirrors intrinsic phase retardation, together with the two new measurements reported in this work, clearly indicate that some physical effect decreases the birefringence per reflection when the mirror reflectivity R increases i.e. when one increases the number of layers used to realize the interferential mirror. Our numerical calculations show that it can be explained with a simple model in which only the layers close to the substrate are birefringent. We could not find any other reasonable configuration giving a trend similar to the experimental one.

Our study cannot unveil the physical origin but it seems to indicate in which part of the mirror the problem resides: the reflecting layers close to the substrate. We believe that it is a crucial piece of information for mirror manufacturers in order to realize birefringence free mirrors or at least to control and minimize the effect.

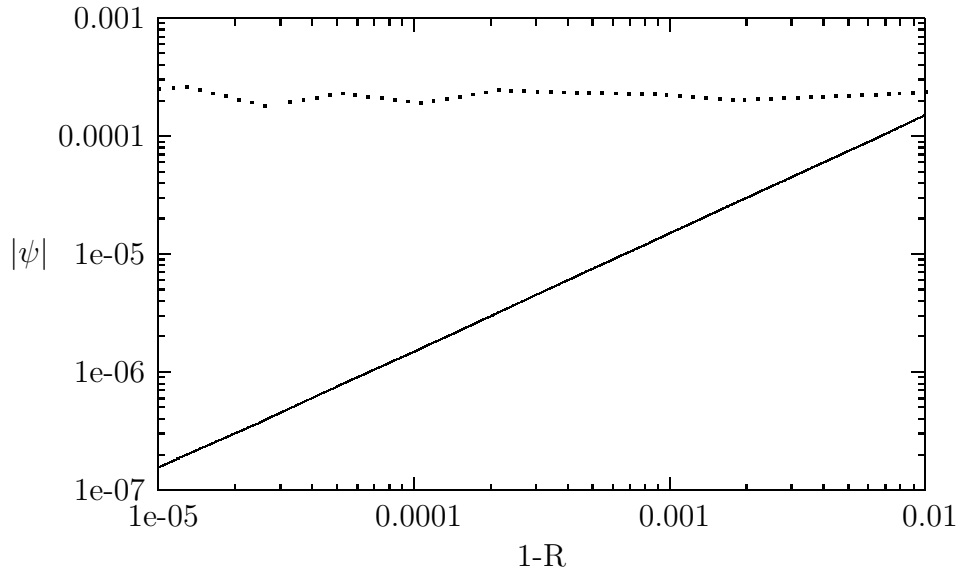
Finally, although experimental data have been obtained by using different mirrors that in principle have not been realized using exactly the same manufacture protocol, we obtain a clear decreasing of the phase retardation per refection as R increases. But to fully understand the origin of interferential mirror phase retardation, we believe that next step should be to study a series of mirrors, all made with the same industrial process, but with different values of reflectivity R.

5 Acknowledgements

This work has been performed in the framework of the BMV project. We thank all the members of the BMV collaboration, and in particular G. Bailly, T. Crouzil, J. Mauchain, J. Mougenot, G. Trénec. We acknowledge the support of the *ANR-Programme non thématique* (ANR-BLAN06-3-139634), and of the *CNRS-Programme National Particule Univers*.

References

1. M.A. Bouchiat, J. Guéna, L. Hunter, and L. Pottier, Phys. Lett. **117B**, (1982) 358-364; M.A. Bouchiat, J. Guéna, and L. Pottier, Phys. Lett. **134B**, (1984) 463-467.
2. S.C. Bennett and C.E. Wieman, Phys. Rev. Lett. **82**, (1999) 2484-2487.
3. R. Cameron, G. Cantatore, A.C. Melissinos, G. Ruoso, Y. Semertzidis, H. Halama, D.M. Lazarus, A.G. Prodell, F. Nezrich, C. Rizzo, and E. Zavattini, Phys. Rev. D **47**, (1993) 3707-3725.
4. S-J. Chen, H-H. Mei, and W-T. Ni, Mod. Phys. Lett. A **22**, (2007) 2815-2831.
5. E. Zavattini, G. Zavattini, G. Ruoso, G. Raiteri, E. Polacco, E. Milotti, V. Lozza, M. Karuza, U. Gastaldi, G. Di Domenico, F. Della Valle, R. Cimino, S. Carusotto, G. Cantatore, and M. Bregant, Phys. Rev. D **77**, (2008) 032006.
6. Phase retardation due to birefringence corresponds to the difference of phase velocities between the two normal modes.
7. M.A. Bouchiat and L. Pottier, Appl. Phys. B **29**, (1982) 43-54.
8. S. Carusotto, E. Polacco, E. Iacopini, G. Stefanini, E. Zavattini, and F. Scuri, Appl. Phys. B **48**, (1989) 231-234.
9. P. Micossi, F. Della Valle, E. Milotti, E. Zavattini, C. Rizzo, and G. Ruoso, Appl. Phys. B **57**, (1993) 95-98.
10. D. Jacob, M. Vallet, F. Bretenaker, and A. Le Floch, Opt. Lett. **20**, (1995) 671-673.
11. W.-T. Ni, Chin. J. Phys. **34**, (1996) 962-966.
12. C. Wood, S.C. Bennett, J.L. Roberts, D. Cho, and C.E. Wieman, Opt. Phot. News **7**, (1996) 54-55.
13. S. Moriwaki, H. Sakaida, T. Yuzawa, and N. Mio, Appl. Phys. B **65**, (1997) 347-350.
14. F. Brandi, F. Della Valle, A.M. De Riva, P. Micossi, F. Perrone, C. Rizzo, G. Ruoso, and G. Zavattini, Appl. Phys. B **65**, (1997) 351-355.
15. J.L. Hall, J. Ye, and L.-S. Ma, Phys. Rev. A **62**, (2000) 013815.
16. G.E. Stedman, Rep. Prog. Phys. **60**, (1997) 615-688.
17. M. Born and E. Wolf, *Principle of Optics* (Pergamon, New York 1980) 55-70.
18. G.J. Sprokel, Appl. Opt. **23**, (1984) 3983-3989.
19. M. Mansuripur, Opt. Phot. News **8**, (1997) 39-44.
20. M.A. Bouchiat and L. Pottier, Phys. Lett. B **62**, (1976) 327-330.
21. E. Iacopini and E. Zavattini, Phys. Lett. B **85**, (1979) 151-154.
22. R. Battesti, B. Pinto Da Souza, S. Batut, C. Robilliard, G. Bailly, C. Michel, M. Nardone, L. Pinard, O. Portugall, G. Trénec, J.-M. Mackowski, G.L.J.A. Rikken, J. Vigué and C. Rizzo, Eur. Phys. J. D **46**, (2008) 323-333.
23. R.W.P. Drever, J.L. Hall, F.V. Kowalski, J. Hough, G.M. Ford, A.J. Munley and H. Ward, Appl. Phys. B **31**, (1983) 97-105.


0.001
0.0001
1e-05
1e-06
1e-07
$|\psi|$
1e-05
0.0001
0.001
0.01
1-R